Empirical Validation of 3T 96 Channel G-factors and Comparison to Ultimate G-Factor

G. C. Wiggins[1], J. R. Polimeni[1], A. Potthast[2], T. Witzel[1], and L. L. Wald[1,3]

[1]NMR Center, Radiology Department, Massachusetts General Hospital, Charlestown, MA, United States, [2]Siemens Medical Solution, Inc, Charlestown, MA, United States, [3]Harvard-MIT Divisions Of Health Sciences and Technology, Cambridge, MA, United States

Introduction: Accelerated imaging performance is one of the primary motivators for the development of receive arrays with higher and higher numbers of elements, typically characterized by the SENSE G-factor Metrics such as the maximum or the mean G-factor for a particular acceleration rate are frequently given as a key characteristic of a particular coil array. In practice, there are many factors which can influence the calculated G-factor map, including the field of view relative to object size (which determines the degree of aliasing), noise level and degree of smoothing in the sensitivity profiles, and whether regularization is used.

High-N receive arrays with up to 96 channels on the head [1] and 128 channels on the body [2][3] have been reported. We have obtained data with a 3T 96 channel head coil which show substantial reductions in G-factor compared to a similarly sized 32 channel coil. The G-factor values calculated for data from these coils can vary widely depending on the acquisition and method of analysis, especially for high acceleration rates. Furthermore, theoretical analysis has shown that there is a fundamental limit (the Ultimate G-factor, G_{ult}) to how low the G-factor can be for a given acceleration rate (R), field of view (FoV) and static magnetic field [4] We have attempted to validate analytically derived G-factor values for these highly parallel arrays by comparing to time series data [5], and to compare these values with the Ultimate G-factor values predicted by theory.

Methods: Data were acquired on a modified Tim Trio 32 channel 3T clinical scanner (Siemens Medical Solutions, Erlangen Germany) using 96 and 32 channel head coils constructed on identical formers[1][6]. A17cm diameter spherical phantom filled with agar and physiological salt concentration was used to avoid fluctuations due to fluid motion. Time series data were obtained for a GRE sequence with TR/TE/Flip = 40/5/20deg, 3mm slice thickness, 128x128 matrix, 165mm FoV and BW=180. The slice was placed just above the center of the phantom, in approximately the position of the Corpus Collusum in a human brain, at a slice position fully surrounded by coil elements. The 165mm FoV was tight on the sample at this slice position, ensuring that the degree of aliasing corresponded to the prescribed acceleration rate. 130 time points were measured for the case of no acceleration, and with various SENSE accelerations applied at the scanner. For each image in the accelerated time series a full k-space sensitivity map was acquired. These high resolution sensitivity maps reduced the edge artifacts which can become prominent at high accelerations. Time series data were acquired with acceleration rates of 2,3,4,5,6,7, and 8. An additional full-k-space single time point scan was acquired, and an identical image with no RF excitation, to generate analytical G-factor maps for comparison to the time series data.

The time series data were analyzed based on the scanner-reconstructed DICOM images. For each series an SNR map was generated by calculating pixel by pixel the ratio of the mean over the standard deviation of that pixel across the time series. The first two images were discarded to allow the acquisition to stabilize and the remaining 128 points were used. G-factor maps were generated by taking the ratio of the unaccelerated SNR to the accelerated SNR divided by the square root of the acceleration rate to account for the SNR loss due to undersampling, or G-factor = $SNR_{unaccel}$ / (SNR_{accel} *SQRT(R)). The G-factor maps are displayed as 1/G-factor to allow all the maps to be represented with the same color scheme. Analytical G-factor maps were generated from the single acquisition and its associated noise acquisition. G-factor maps were generated using smoothed sensitivity profiles (utilizing 25% of the phase encode lines to smooth out high frequency variations) and for the "raw" case where the full k-space images from the individual coils were used as the sensitivity maps. Ultimate G-factor values appropriate to this B_0 field and FoV were approximated by interpolating values given in Ref 4.

Results: The empirical G-factor maps (Fig.1) agree quite closely with the analytical maps, particularly for higher accelerations. When no smoothing is used in the analytical G-factor calculation, noise in the data caused the G-factors to be underestimated. The analytical maps with smoothing correspond very closely to the empirical maps, lending confidence to these G-factor numbers. In Fig. 2 the maximum G-factor in each map is plotted for the various methods. The empirical and smoothed analytical lines lie very close to each other, and are not much higher than the Ultimate G-factor, shown in black. The "raw" analytical maps underestimate the G-factor at high rates so much that they eventually appear to be lower than the Ultimate G-factors, further confirming the bias that can be introduced by noise in the sensitivity maps. For comparison, 32 channel data are shown, demonstrating the G-factor improvement with the move to 96 channels.

Conclusions: Empirical data and careful comparison to the Ultimate G-factor have demonstrated that the 96 channel coil appears to approach, but not quite reach, the Ultimate G-factor. The experimental setup did not, however, correspond precisely to the formulation of the Ultimate G-factor in Ref 4. The data we present here are for a slice position away from the center of the phantom. While the FoV is 165mm, there are coils on the dome of the coil which may be closer than ½ the FoV from the imaging plane in the through plane direction. It is probable though that there is unlikely to be much benefit in moving to higher numbers of elements for head coils at 3 Tesla. The G-factor benefits of 96 compared to 32 channels is however clear. This is further demonstrated in the highly accelerated images in Fig. 3

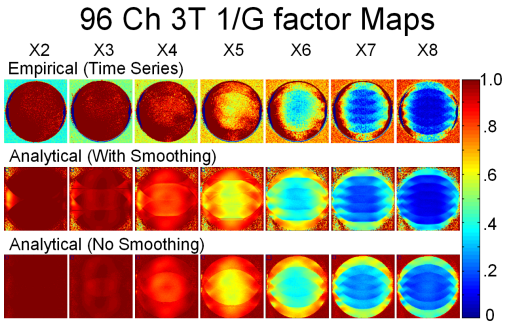

Fig. 1 Maps of 1/G for the 3T 96 Channel coil.

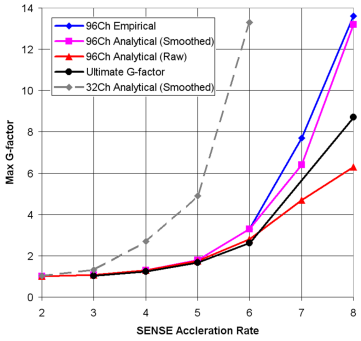

Fig. 2. Maximum G-factor as a function of acceleration rate for the various methods, compared to the Ultimate G-factor for 3 Tesla and 165mm FoV.

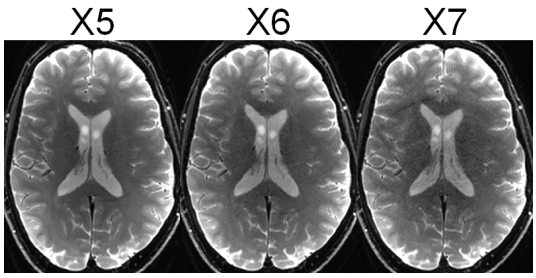

Fig. 3. GRAPPA accelerated spin-echo EPI images showing the acceleration capability of the 96 channel coil

[1] Wiggins GC et. al. Proc ISMRM 2007 [2] Schmitt M, et.al. Proc ISMRM 2007 p245 [3] Hardy C, et.al. Proc ISMRM 2007 p244 [4] Wiesinger F, et.al. Magn. Reson. Med. 2004; **52:** p376-390 [5] Ohliger M, et.al. NMR Biomed. 2006; **19:** p300-315 [6] Wiggins GC et. al. Mag Reson Med. 56(1):216-223 (2006)